Hindawi
Advances in Civil Engineering
Volume 2024, Article ID 1177939, 17 pages
https://doi.org/10.1155/2024/1177939

Research Article

Effect of Elevated Temperature on Microstructural and Durability Properties of High-Strength Concrete-Containing Eggshell

Samuel Sisay Asgedom [1,2] **and Bahiru Bewket Mitikie** [3]

[1]*Department of Construction Technology and Management, Institute of Technology, Debre Berhan University, Debre Berhan, Ethiopia*
[2]*Department of Civil Engineering, College of Architecture and Civil Engineering, Addis Ababa Science and Technology University, Addis Ababa, Ethiopia*
[3]*Department of Civil Engineering, Adama Science and Technology University, Adama 1888, Ethiopia*

Correspondence should be addressed to Samuel Sisay Asgedom; samuel.sisaya@aastustudent.edu.et

Received 1 September 2023; Revised 9 November 2023; Accepted 30 January 2024; Published 14 February 2024

Academic Editor: Afshar A. Yousefi

Researchers have recently discovered that eggshell contains a significant amount of calcium carbonate through the characteristics of both fresh and hardened concrete by partially substituting cement with eggshell powder (ESP) at room temperature. The objective of this experimental investigation was to examine the microstructural and durability characteristics of high-strength concrete exposed to elevated temperatures using ESP as partial cement replacement. The impact of elevated temperature intensity (200, 400, 600, and 800°C) for one hour of exposure on the specimens and natural air-cooling method was studied. Various ESP cement blending percentages (0%, 5%, 10%, and 15%) were examined through different microstructural and durability tests such as workability, fire resistance, scanning electron microscopy (SEM), X-ray diffraction (XRD), Fourier transform infrared spectroscopy, and 3D optical surface profiler, air content tests, ultrasonic pulse velocity, weight loss, spalling and color changes, water absorption, and acid attack experimental tests. According to the findings, the amount of ESP exceed 5% replacement reduces the workability of fresh concrete mixtures. The best performance was reached by a mixture comprising 5%ESP specimens, with values of 63.41 and 64.07 MPa at ambient and 200°C, respectively. SEM results of 5%ESP at 200°C illustrate a decrease in the occurrence of pores and act as a bridge to form crystals between CH and C—S—H. The XRD result also indicates a high amount of jennite (C—S—H gel) was formed at 200°C due to the melting of ESP, which densifies the crystal of C—S—H. Regression analysis provided a more reliable expression for the relationship between the residual compressive strength and UPV with R^2 values of 0.9833 and 0.9966 for control and 5%ESP mixes, respectively. As a result, it was determined that concrete with 5%ESP as a partial cement replacement performs better over time than control concrete and has the potential to be used in construction.

1. Introduction

The production of ordinary Portland cement (OPC), a key component in the fabrication of concrete, directly contributes to the depletion of natural resources and the ongoing emission of CO_2 into the environment. A similar amount of CO_2 is released into the atmosphere per ton of cement production [1]. Numerous studies show that 5%–8% of the total global manufactured CO_2 emissions are attributable due to the production of cement [1–5]. Due to these reasons, attempts have been made to find more readily available, environmentally friendly materials that can partially replace cement. Because of their pozzolanic characteristics, agricultural wastes like eggshell powder (ESP), bone ash powder, coconut shell, and rice husk ashes are frequently utilized in the manufacturing of concrete and mortar [6].

Eggshell is an excellent substitute for cement since it contains about 93.7% $CaCO_3$ [7]. The eggshell cover, which makes up around 11% of the total weight of the egg, comprises calcium carbonate, phosphate, magnesium carbonate,

and organic compounds in proportions of 94%, 1%, 1%, and 4%, respectively. As a result, we can conclude that eggshell shares chemical properties with cement's limestone. About 5 g of ESP can be produced from a single eggshell [8].

It has recently been discovered that ESP, an agricultural waste product that is dumped into the environment, is rich in calcium and has the same chemical composition as limestone. Additionally, it has been discovered that using specific replacement can enhance the qualities of mortar and concrete, such as compressive strength, flexural strength, split tensile strength, and workability [9]. ESP was used in an experimental investigation to substitute a portion of the cement, and Kumar et al. [10] examined the impact on the concrete's strength. Additionally, eggshells can be utilized to shield against radiation. The use of such concrete material was highly advocated as a way to stop radioactive materials from escaping [11]. However, just a few experiments have been conducted to determine whether the ESP mixed cement in high-strength concrete (HSC) will hold up over time when subjected to high temperatures.

Significant advancements, such as design flexibility and freedom of economical resource utilization, have been made recently as a result of the increased implementation and production of HSC. Due to its high modulus of elasticity, early strength development, high tensile strength, low creep, and low shrinkage, concrete receives a lot of attention in fields other than high-rise buildings, such as bridge construction, precast, and prestressed concrete [12].

Concrete constituent elements (such as kind of aggregate, cement paste characteristics, adhesion of aggregate and cement paste, and thermal compatibility between components of the composite) and environmental factors are the key factors affecting the strength of concrete in a heated state (heating rate, length of exposure to optimum temperature, cooling rate, and loading conditions) [13]. Elevated temperatures have negative effects on cement paste, which is the binding material in concrete. Understanding the effects of elevated temperature on cement paste is crucial for assessing the performance and durability of concrete structures exposed to fire or other elevated temperature environments. Having a great understanding in such areas helps engineers and designers to make decisions regarding material selection, structural design, and fire-resistant measures to ensure the safety and integrity of concrete structures in such conditions [14]. Free and bound water from the C—S—H gel evaporates at temperatures between 100 and 300°C. When the temperature exceeds 300°C, there is a 15%–40% drop in strength. The dihydroxylation of Ca $(OH)_2$ takes place at a temperature of 500°C with a reduction in strength of 55%–70%. The internal strains and microcracks that are created through the cementing material increase as a result of the dehydration of calcium silicate hydrate and the associated thermal expansion [15].

The behavior of concrete at elevated temperatures is influenced by factors such as the speed of temperature rise and the type and stability of the aggregate. Unexpected changes in temperature can cause spalling and cracking due to thermal shock, and aggregate expansion can also damage concrete and lead to degradation in the compressive strength of concrete [16].

It is common that calcium hydroxide losses its water and leaves calcium oxide at around 400–500°C. If this calcium oxide is wetted after cooling or exposed to moist air, it rehydrates to calcium hydroxide accompanied by a large expansion in volume. This may derange concrete that has withstood fire hazards without actual disintegration. Exposure to sustained temperatures of 650–820°C makes the concrete easily breakable and porous and usually can be taken apart with fingers after cooling. However, total dehydration is only complete at a temperature of 800°C or above. Here, most of the decompositions are irreversible, so damage to concrete is essentially permanent [15]. There is no common or conventionally accepted opinion with researchers on the properties of concretes, particularly in the temperature range of 100−300°C, whereas for temperatures above 300°C, there is uniformity in opinion concerning a decrease in mechanical characteristics [17].

The service period of a construction building exposed to elevated temperature is another concern when studying the fire resistance of building materials, as the effect of the thermal attack on durability is still not understood [18]. It is crucial to know how elevated temperatures affect concrete's physical characteristics [19]. A concrete structure could suffer significant damage during a fire because temperatures inside buildings can rise to up to 1,100°C, and in tunnels, can even reach 1,350°C [20]. The following list includes the primary phases that make up the microstructure of hydrous cement paste: Ettringite, monosulfate, unhydrated cement particles (UH), air spaces, calcium hydroxide (CH), calcium silicate hydrate (C—S—H), and calcium hydroxide (C—S—H) [21]. Due to their reliance on material porosity, permeability, and pore size distribution, cementitious materials' pore structure has a substantial impact on qualities, including strength and durability [22].

Due to the high heat, Ca ions, siloxanes, and water molecules form a variety of teams in the C—S—H gel structure that contribute to bonding between surfaces or within the bed of tobermorite material that is partially crystallized. The strength, stiffness, and creep qualities of the cement paste are determined by the hydrogen bonds formed between the water present in the layers (gel water) and other groups [23]. Even before the temperature hits 100°C during heating, ettringite begins to break down. Progressive C—S—H gel dehydration starts as soon as the fabric begins to heat up. It is important to note that the structure of the cement paste is partially destroyed as a result of dehydration at a temperature of 105°C, which is typical for the drying of materials [24].

However, a lot of earlier research likewise disregarded the impact of high temperatures on concrete's attributes. A clear understanding and knowledge of how to take any remedial action before structural failure and damage will also be provided by having advanced information about the behavior of concrete after elevated temperatures collected through various microstructural and durability tests. Currently, most of civil infrastructures use HSC; so due to the economy and sustainability of nonrenewable materials like cement, it is

Figure 1: Eggshell powder. Source: Own work, 2022.

better to replace cement using ESP as partial replacement during the production of such concrete. Since it has a similar chemical composition as lime and can withstand elevated temperatures, but previous studies were focused on using ESP as a partial replacement on conventional (normal) strength concrete, not in HSC. It is, therefore, through various physical, microstructural, and durability tests, the study was examined.

2. Materials and Methods

2.1. Materials. The materials used for the production of concrete were ordinary Portland cement, coarse aggregate, fine aggregate, water, ESP, and superplasticizer.

For this study, ordinary Portland cement of grade 42.5N with a specific gravity (SG) of 3.16, produced by the Mugher cement factory, was employed. This cement complies with C150/C150M (2011) and is an ASTM Type I cement [25]. The coarse aggregate used had a nominal size of 19 mm, and the fine aggregate ranged in size from 75 m to 4.76 mm, fitting ASTM C33 [26]. The eggshell used in this investigation was gathered from the Addis Ababa-based MAM Bakery food processing facility. After being washed and cleaned, they were dried in an oven at 105°C for 24 hr before being ground into a powder. The powder is sieved through a 150-m sieve size after the eggshell has been ground. A high-range water-reducing superplasticizer (Sika Viscocrete) that complies with ASTM C-494/C-494M specifications was utilized as an admixture. According to ASTM C-1602, potable water is utilized as a mixing and curing ingredient (2012). Figure 1 illustrates an eggshell that is cleaned, oven dried, and grinded to powder.

The chemical compositions of egg-shell powder are shown in Table 1.

The particle size distribution of aggregates was conducted as per ASTMC-136 (2013), and the result is presented in Figures 2(a) and 2(b).

Table 1: Chemical composition of ESP.

Elemental oxide	Percentage (%)
SiO_2	3.38
Al_2O_3	<0.01
Fe_2O_3	<0.01
CaO	49.22
MgO	0.60
Na_2O	<0.01
K_2O	<0.01
P_2O_5	0.30
H_2O	0.73
LOI	45.82

Source: Own work, 2022.

2.2. Methods

2.2.1. Raw Material Characterization. Since the characterization of the raw material plays a vital part in the manufacture of concrete's quality control system, it was carried out appropriately prior to preparation. Thus, the physical attributes are density, moisture content, SG, and water absorption. Both the fine and coarse aggregates were tested. X-ray fluorescence was used to study the chemical composition of ESP in order to comprehend the oxide compound of ESP (XRF).

2.2.2. Mix Proportion. To produce consistent concrete, the ingredients must be well-mixed. The mass should become homogeneous, color-uniform, and consistent as a result of the mixing. By using ACI 211 as a guide, an HSC mix ratio of 1 : 1.22 : 1.57 cement, fine aggregate, and coarse aggregate, together with a water–cement ratio of 0.33, was chosen for the investigation. The percentages at which cement was substituted with ESP were 0%, 5%, 10%, and 15%. The materials list for one cubic meter of C-50-grade concrete is shown in Table 2, and the proportions are made in line with ACI 211 [27].

2.2.3. Sample Preparation and Curing Condition. Using typical cubical molds with dimensions of $100 \times 100 \times 100\ mm^3$, casting for a fire resistance test. To ensure a homogeneous mixture, the necessary volumes of the mix's component parts were measured and properly combined. A common pan-style mixer was used for mixing. A vibrating compactor was used to remove trapped air after the concrete was placed on the mold. Cubes were demolded after 24 hr, which is allowed to get hardened, and put in the curing tank. Those curing tanks were previously cleaned and filled with potable water up to the

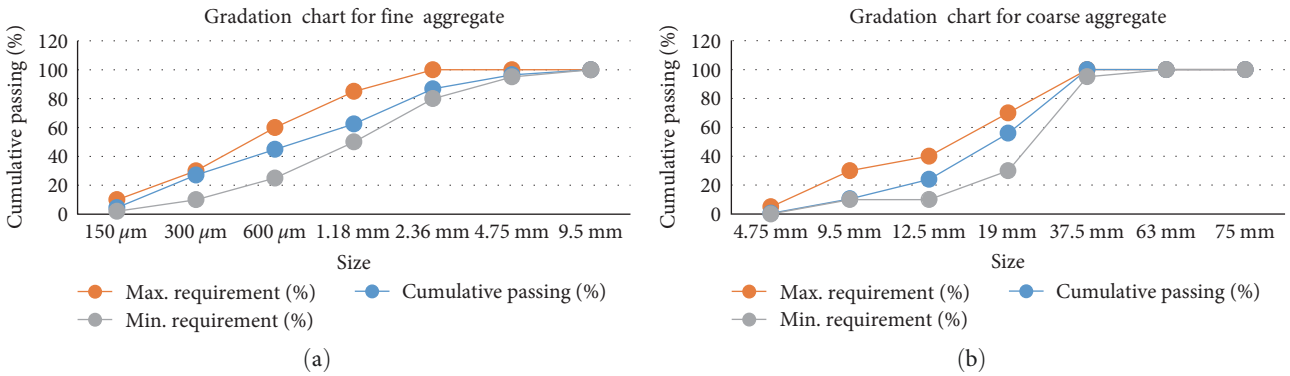

Figure 2: Gradation chart for fine and coarse aggregates ((a) = fine aggregate, (b) = coarse aggregate). Source: Own work, 2022.

Table 2: Mix proportion for each mix.

Mix code	Mix proportion	Cement (kg)	ESP (kg)	Sand (kg)	CA (kg)	Water (kg)	SP (ml)	w (cm)
M_0	100%OPC	21	0	25.68	32.85	7.2	63	0.33
M_1	95%OPC + 5%ESP	19.95	1.05	25.68	32.85	7.2	63	0.33
M_2	90%OPC + 10%ESP	18.9	2.1	25.68	32.85	7.2	63	0.33
M_3	85%OPC + 15%ESP	17.85	3.15	25.68	32.85	7.2	63	0.33

Source: Own work, 2022.

Figure 3: Sample cubes and curing mechanism. Source: Own work, 2022.

level where specimens sunk fully. The curing was conducted at room temperature level of 25 ± 2 for 28 days. However, samples made for the acid attack test were submerged in tanks containing water with a 3% concentration of sulfuric acid for 56 days before being assessed for the level of deterioration. Figure 3 presents the sample cubes and curing mechanism used.

2.2.4. Workability Test on Fresh Concrete. Slump tests were carried out on the fresh concrete to determine the workability of each mix. The tests were done in accordance with BS 1881–102 procedures for slump tests [28]. Figure 4 shows the slump test apparatus and sample slump result for mix 1 (control mix).

2.2.5. Air Content Test. Testing for air content is advised for the purpose of profile characterization of the specific concrete batch, even if the concrete is not subject to freeze/thaw cycles. About 1%–2% of nonair-entrained concrete has air trapped inside of it on average, and various admixtures may unintentionally trap even more air [29]. Additionally, by looking at the presence of air, which is directly related to strength, this test is useful in estimating the longevity of concrete. The pressure method (Type B concrete air meter), one of the known types of air content test methods, was therefore used in this study. Figure 5 shows the apparatus used to measure the air content in each fresh mix.

2.2.6. Unstressed Residual Compressive Strength Test. Compressive strength, which is the main durability property of concrete, is affected when the hydration process of Portland cement is attacked due to high temperatures. According to BS 1881-116, a residual compressive strength test was performed [30]. Using an electric furnace, the concrete cube specimens were heated at average rates of 10°C/min to temperatures of 200, 400, 600, and 800°C. Figure 6 illustrates how the temperature was raised in accordance with the ISO-834 fire curve.

Figure 7 shows the images of the electric furnace and the compressive strength testing machine.

At laboratory temperature (25 ± 2°C), the concrete samples were allowed to cool naturally in the air. Then, for each concrete specimen, the residual weight, spalling, UPV (this

(a) (b)

Figure 4: (a) Slump test apparatus and (b) slump for sample M1. Source: Own work, 2022.

Figure 5: Air content (pressure method) testing equipment. Source: Own work, 2022.

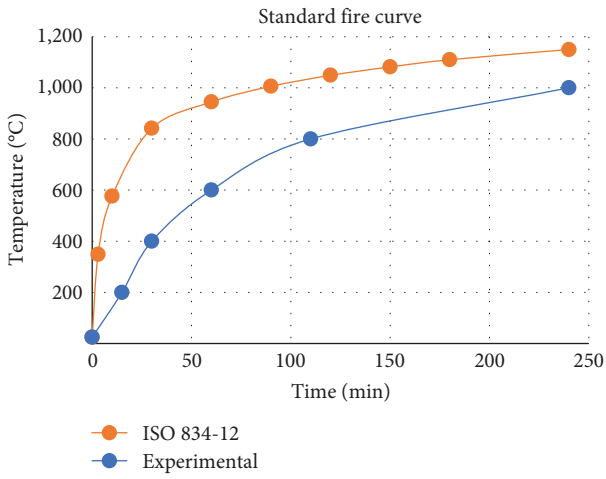

Figure 6: Time–temperature curve of the electrically controlled furnace. Source: Own work, 2022.

test is used to investigate the quality and homogeneity of concrete through determination of pores and cracks), and cube compressive strength were noted. The morphology and microstructure of the concrete samples were examined using scanning electron microscopy (SEM: provides morphological information within crystalline calcium hydroxide and calcium silicate hydrate), X-ray diffraction (XRD: provides mineralogical composition of the concrete mix), Fourier transform infrared spectroscopy (FTIR: this microanalysis test is used for quantifying functional grouping the degree of oxidation through identifying chemical composition/properties. A change in the characteristics pattern of absorption bands clearly indicates a change in the composition of the material or the presence of contamination), 3D optical surface profiling (this test checks the surface crack, depth, shape, form, and surface depression), and differential scanning calorimetry (DSC: help to examine the thermal analysis of an ESP to find the change in both physical

(a) (b)

Figure 7: (a) Electric furnace (3,000°C) and (b) compressive strength testing machine. Source: Own work, 2022.

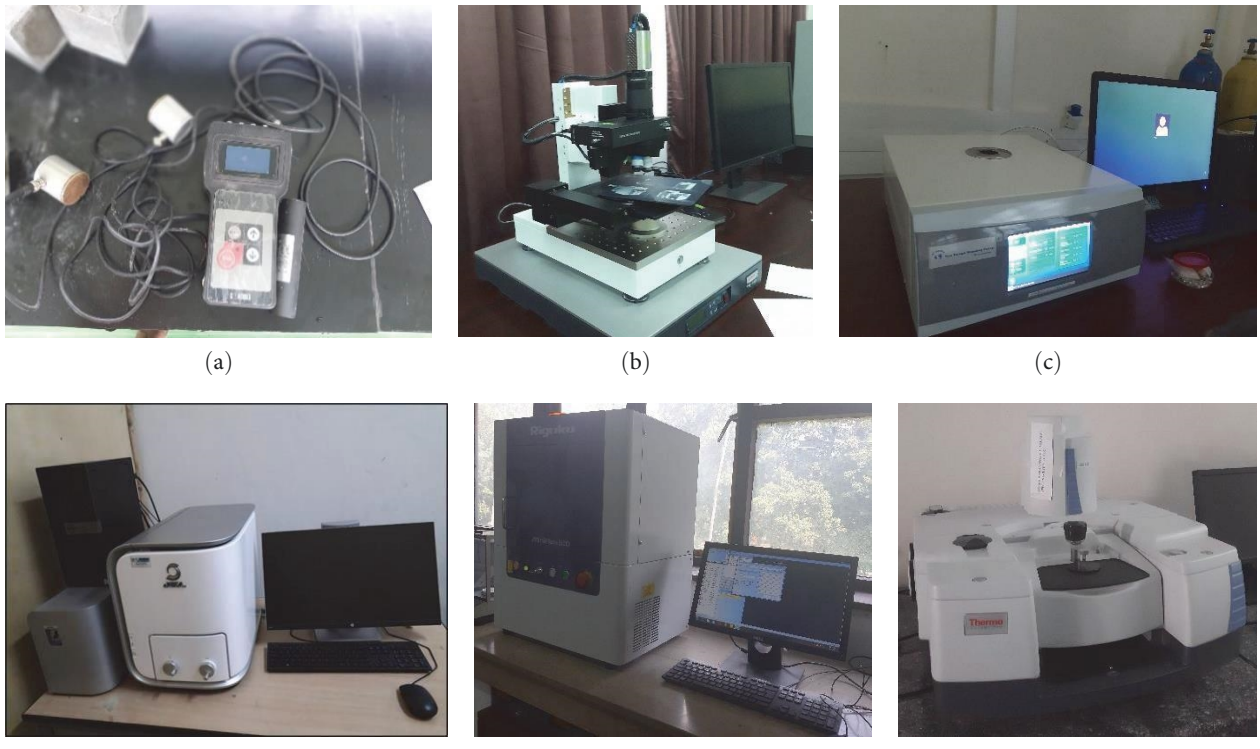

(a) (b) (c)

(d) (e) (f)

Figure 8: (a) Ultrasonic pulse velocity testing equipment, (b) 3D optical microscope, (c) differential scanning calorimetry testing machine, (d) scanning electron microscope (JCM-6000, (e) MiniFlex benchtop X-ray diffractometer, and (f) FTIR testing machine. Source: Own work, 2022.

and chemical within the sample due to temperature. The heating rate was increased at 10°C/min over the range of 25.4–700°C) at both room and elevated temperatures for Control (0%ESP) and 5%ESP mix samples only at an ambient and 200°C. The experimental program also included water absorption and acid attack tests. Figure 8 illustrates the equipment used to evaluate and analyze the microstructural properties on selected samples.

3. Experimental Results and Analysis

3.1. Influence of ESP on the Workability of Concrete. The slump test was used to measure the impact of ESP on the workability of fresh concrete. At a constant water-to-cement ratio of 0.33, the slump height fell as more ESP was substituted with cement. This may have been caused by ESP's high water absorption rate, which depletes the water supply and

Table 3: Slump values of concrete specimens.

ESP content (%)	Slump (mm)	Slump type
0	78	True slump
5	75	True slump
10	70	True slump
15	62	True slump

Source: Own work, 2022.

Table 4: Air content of fresh concrete mix.

Concrete mix	Air content (%)
0%ESP	2.1
5%ESP	2.7
10%ESP	3.8
15%ESP	4.2

Source: Own work, 2022.

limits flowability [31]. However, according to BS1881-102, the fresh concrete for all combinations was categorized as having a true slump (i.e., 75 ± 25 mm). Table 3 presents the results of the downturn.

3.2. Air Content Test Result. Because of uncontrollable factors during the batching, mixing, and placement of fresh concrete, each concrete mix contains entrapped air. For the control mix, the air content was about 2.1% and gradually increased up to 4.2% for the rest of the ESP blended mix concrete. This shows that an ESP has pores, and those pores entrap air from the environment. Therefore, this shows the strength and durability also deteriorate as the amount of ESP increases. Table 4 indicates the air content of each mixture, as shown below.

3.3. Spalling and Surface Color. During the fire testing, there was no noticeable explosive spalling in the ESP-containing concrete cubes. This result confirmed the idea that ESP can considerably increase concrete's resistance to spalling at high temperatures. The low melting point of ESP may be to blame for these phenomena. The melting range for the powder is 72–337.3°C. The bed of powder serves as an extra channel for gases as it melts and is partially absorbed by the matrix. Figure 9 illustrates the effect of elevated temperature on the surface texture of different concrete mixes.

3.4. Mass Loss. The weights of sample cubes were measured before and after exposed to elevated temperatures in order to assess weight loss. All samples' mass loss is expressed as a ratio of their initial mass at room temperature to their final mass following exposure to a certain increased temperature. Theoretically, the dissolution of calcareous aggregates, release of carbon dioxide (CO_2), and sloughing off of the concrete surface might be blamed for the mass loss in the concrete specimen at elevated temperatures, altering the mechanical properties of the concrete. Furthermore, due to the vaporization of free water in the calcium silicate hydrate (C—S—H) gel and the decomposition of calcium hydroxide Ca (OH)2, the cement matrix loses its binding properties [32]. Figure 10 depicts the effects of high temperature on the mass loss of control and ESP-blended concrete samples.

3.5. Residual Ultrasonic Pulse Velocity (UPV). UPV, which is a nondestructive test, was used to assess the quality, homogeneity, and presence of pores and cracks. As can be seen, the ESP's presence has no appreciable impact on the UPV values of the concrete. The UPV values of the concrete mixtures were somewhat high at ambient temperature; however, lower values were seen in all test specimens at higher temperatures. In terms of concrete quality [33], the higher UPV values for the control mix and the 5%ESP mix at room temperature were 4,230 and 4,380 m/s, respectively. It is possible that the melted ESP form serves as a filler for crystal pores because a concrete sample containing 5%ESP has a greater UPV at 200°C with an average of 4,320 m/s. The fluctuations in the UPV of the ESP-concrete mixtures exposed to the specified temperatures are shown in Figure 11.

3.6. Residual Compressive Strength. The findings showed that adding ESP reduced the concrete's compressive strength by more than 5% when it was at room temperature. The inclusion of ESP at a volume percentage of 10% reduced the compressive strength by 10.6% when compared to the value of the control mix (concrete without any ESP). The concrete with 15%ESP showed a further reduction in compressive strength of 27.3% compared to OPC concrete. The sluggish hydration and limited pozzolanic activity of ESP were blamed for the reduction, which contradicted the rise in concrete's compressive strength [34]. Except for 5%ESP, all mixes' compressive strengths decreased from their strength readings at room temperature by 3%–8% after heating up to 200°C. The production of dense crystal C—S—H, when melted ESP serves as a void filler, may result in an improvement in strength at 5% ESP mix. Figure 12 depicts the experimental findings of residual compressive strength of concrete mixtures at ambient temperature and after heating to 200, 400, 600, and 800°C in an air-cooled regime. Table 5 presents the average residual compressive strength of each mixture.

The residual compressive strength of concrete mixtures is shown in Table 5.

3.7. Relationship among the Residual Compressive Strength and UPV. It was observed that the UPV values could be correlated with the corresponding residual cube compressive strength. The obtained result of residual cube compressive strength was used as a response factor with the residual UPV values as their predicator parameter. To correlate the experimental data, the linear regression method was employed, resulting in Equations (1) and (2), with R^2 values of 0.9833 and 0.9966 for samples with 0%ESP and 5%ESP, respectively, which signified excellent positive confidence for the relationships between UPV and residual compressive strength.

The equations are presented as the following:

$$f_{\mathrm{rcu}} = 0.0443V - 124.89 \ (R^2 = 0.9833), \quad (1)$$

$$f_{\mathrm{rcu}} = 0.0333V - 82.229 \ (R^2 = 0.9966), \quad (2)$$

where f_{rcu} is the residual cube compressive strength (MPa), and V signifies the residual UPV (m/s) at high temperatures.

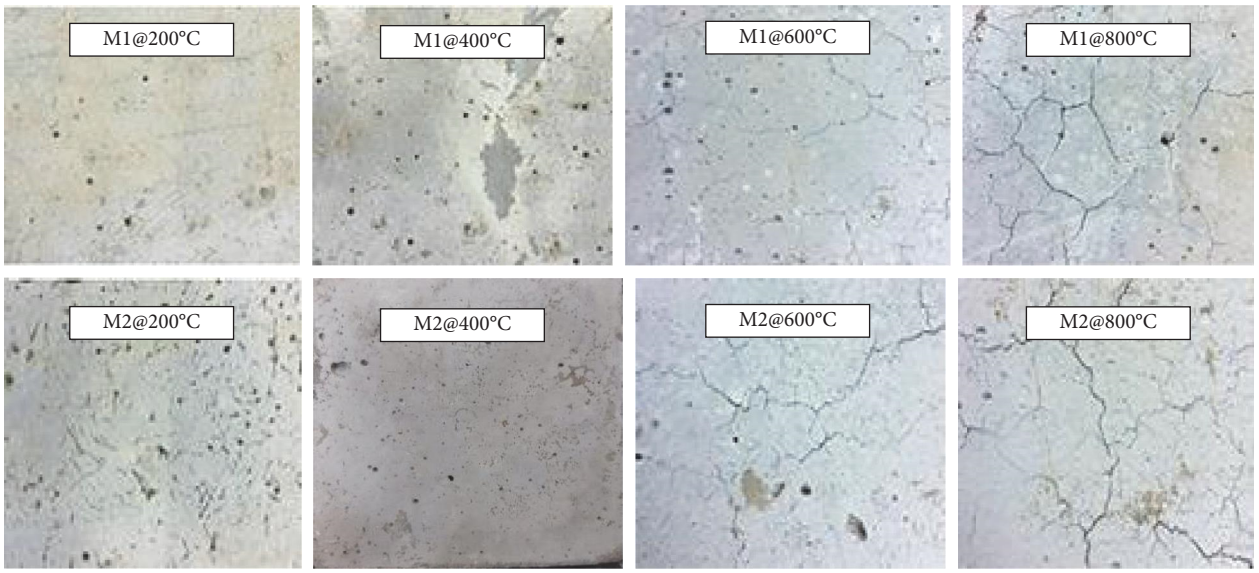

Figure 9: Surface texture of the concrete specimens after exposing to high temperatures. Source: Own work, 2022.

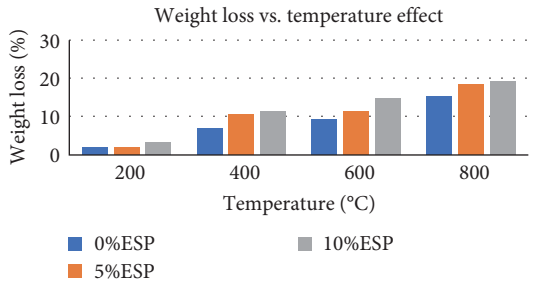

Figure 10: Mass loss of different concrete mixtures due to elevated temperature. Source: Own work, 2022.

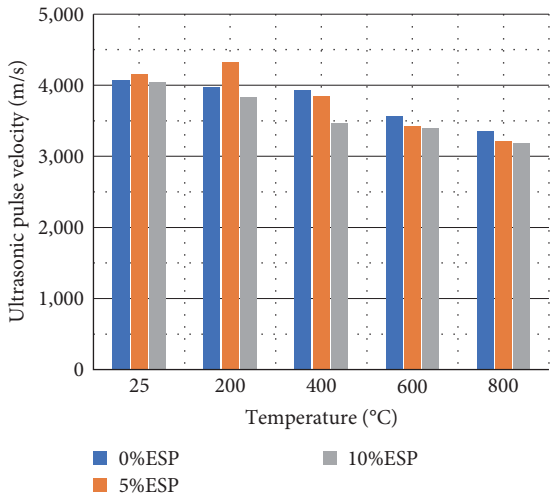

Figure 11: Variation in UPV values of concrete mixtures due to elevated temperature. Source: Own work, 2022.

Figure 13 illustrates a good relationship between the residual compressive strength and UPV values of the control (0%ESP) and 5%ESP concrete mixtures at high temperatures.

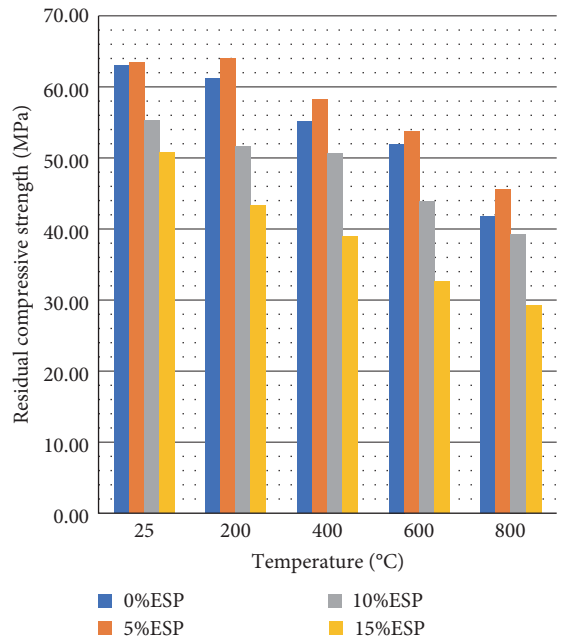

Figure 12: Residual compressive strength of concrete mixtures. Source: Own work, 2022.

3.8. Water Absorption. One important test to measure the durability of concrete is water absorption. Mohd Arif et al. [31] claim that higher ESP substitution levels cause an increase in the amount of water absorption. In comparison to the control mix, water absorption of sample specimens increased by 0.56%, 0.7%, and 2.7% after 10 min, 0.45%, 1.05%, and 3.45% after 30 min, and 0.5%, 1.65%, and 4.5% after 60 min of immersion. The replacement levels of ESP were 5%, 10%, and 15% of the total cement weight. As a result, the 5%ESP mix outperforms the other mixes and has durability strength that is comparable to the control

Table 5: Average residual compressive strength of concrete mixtures.

	25 ± 2°C	200°C	400°C	600°C	800°C
0%ESP	62.99 MPa	61.14 MPa	55.13 MPa	51.97 MPa	41.74 MPa
5%ESP	63.41 MPa	64.07 MPa	58.27 MPa	53.73 MPa	45.57 MPa
10%ESP	55.26 MPa	51.60 MPa	50.69 MPa	43.90 MPa	39.29 MPa
15%ESP	50.76 MPa	43.36 MPa	38.90 MPa	32.59 MPa	29.19 MPa

Source: Own work, 2022.

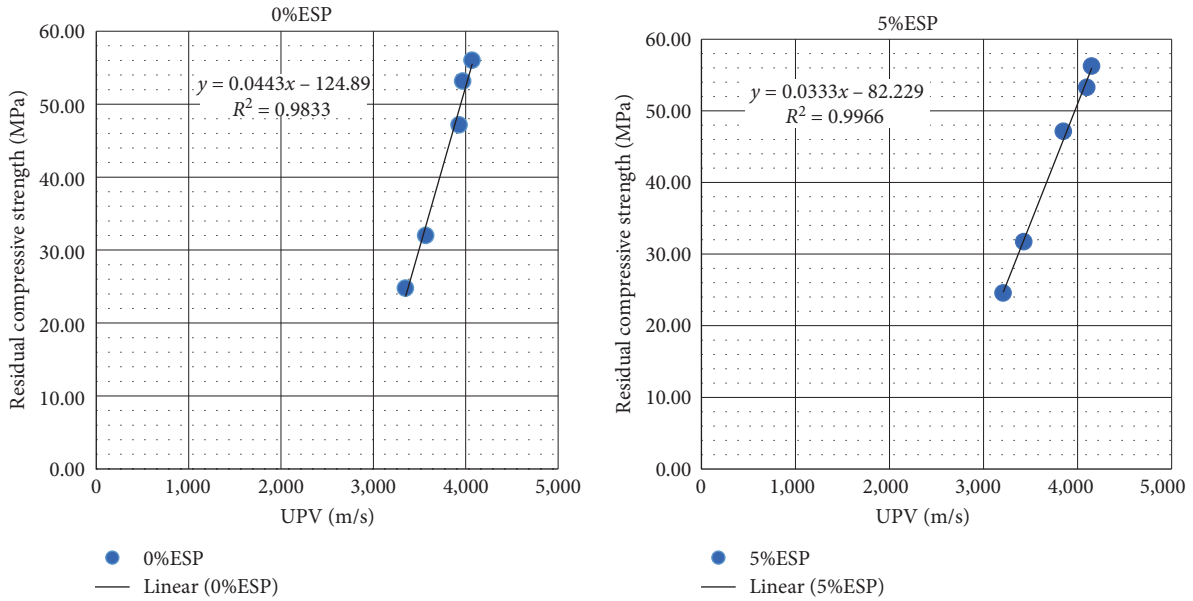

Figure 13: Correlation among residual compressive strength and UPV for 0% and 5%ESP mixtures. Source: Own work, 2022.

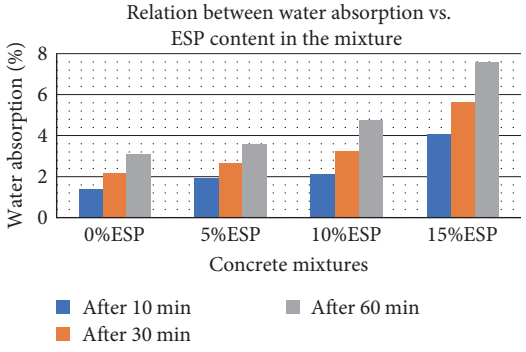

Figure 14: Effect of ESP on concrete water absorption characteristics. Source: Own work, 2022.

mix. Figure 14 shows the effect of excess in ESP on the concrete water absorbability.

3.9. Acid Attack. Concrete specimens with and without ESP were made in order to examine the impact of sulfuric acid attack. Following 28 days of curing, those samples were heated to 25, 200, and 400°C then cooled for three hours. After cooling, the sample specimens were submerged for 56 days in a 3% solution of H_2SO_4 (sulfuric acid). In all samples of concrete mixture, the presence of an acid solution significantly changes the color. This scenario also supported a decline in surface smoothness and a decrease in concrete strength. Figure 15 illustrates the effect of sulfuric acid concentration on the surface of sample cubes.

The imposed elevated temperature and acid concentration reduce the strength of the 5%ESP sample concrete by 13.47% and 13.25% at 25 and 200°C, respectively. This shows that high temperature and acid concentration have a great impact on the depreciating durability property of concrete. Table 6 represents the value of selected mixes exposed for a specified elevated temperature in accordance with acid concentration.

3.10. 3D Optical Surface Analysis. The Meta-20 3D optical surface profiler was used for the experiment. Since this test is a crucial tool for determining surface integrity, the majority of the inquiry was concentrated on identifying surface cracks and the apparent loss of binding between the paste and aggregate owing to high temperatures. However, after exposing the test concrete specimens to temperatures of 400°C and higher, a sizable break could be noticed. This situation demonstrates that concrete materials alone or when combined with ESP are unable to endure fire or extreme temperatures exceeding 400°C. The experimental inquiry in Figure 16 demonstrates the direct proportion between crack and temperature, leading to the conclusion that cracks are indicators of deteriorating concrete material strength.

The concrete sample containing 5%ESP has a better surface bond than the control mix, as shown in Figure 16, and

Figure 15: Sample concrete specimens color change due to sulfuric acid solution. Source: Own work, 2022.

Table 6: Residual compressive strength due to sulfuric acid attack test result.

ESP (%)	After 28 days of water curing (MPa)			After 56 days of acid curing (MPa)		
	@25°C	@200°C	@400°C	@25°C	@200°C	@400°C
0	62.99	61.14	55.13	51.08	49.12	44.30
5	63.41	64.07	58.27	54.87	55.58	51.02
10	55.76	51.60	50.69	47.55	41.54	37.58

Source: Own work, 2022.

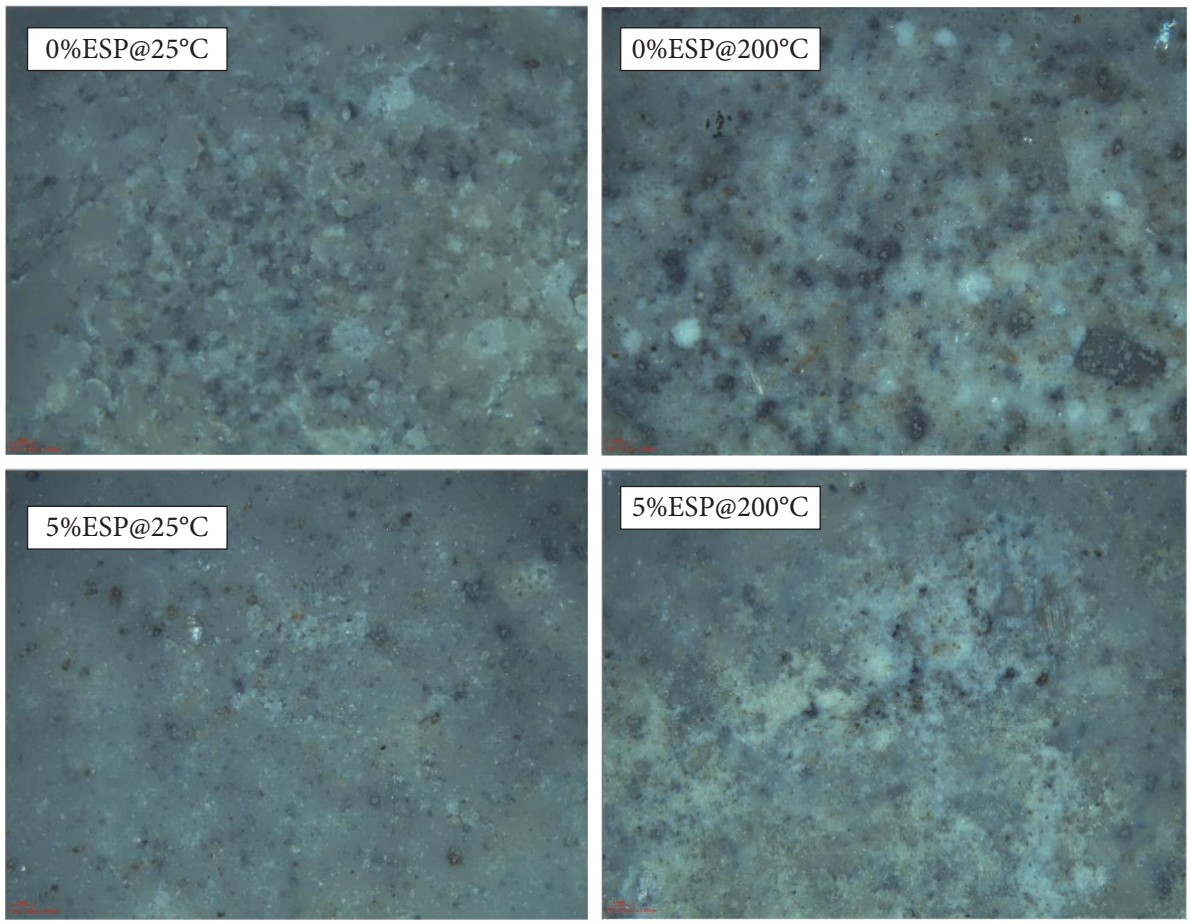

Figure 16: 3D Optical surface profiler image for sample concrete specimens. Source: Own work, 2022.

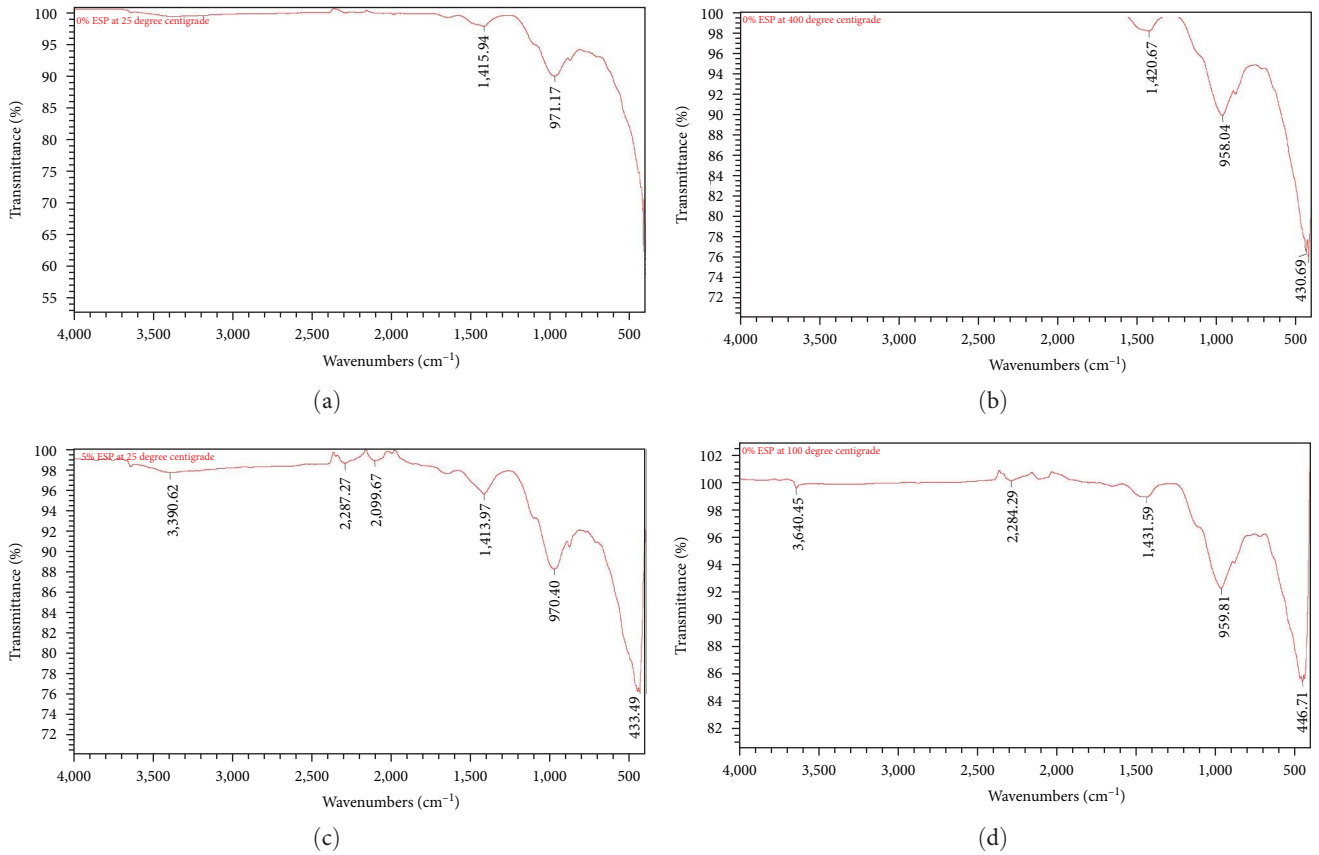

Figure 17: FTIR spectrum for mixtures 0%ESP@25°C (a) and 200°C (b), and 5%ESP@25°C (c) and 200°C (d). Source: Own work, 2022.

the development of thick calcium hydroxide may be the result of the presence of silica and $CaCO_3$. Here again, we may determine the surface roughness by simply comparing the Ra (average roughness or arithmetic mean deviation) values of those sample specimens. The Ra values under the circumstances of 0%ESP at ambient (25 ± 2) and 200°C were 14.9 and 16.16, respectively, while the Ra values for a mix with 5%ESP were foster good and 11.86. Using this information, one may quickly determine the surface roughness of samples by comparing the amplitude parameter seated by ISO4287:1997.

3.11. FTIR Analysis. The experiment was done on particular concrete samples with ESPs of 0% and 5%. The samples for each combination were heated to temperatures of 25 and 200°C before the appropriate sample powder was made for testing in order to identify the compounds' functional groups and to look for temperature-related variations. At both 25 and 200°C, the first mixture had no discernible free water. The second mix, however, contains a substantial amount of free water throughout the mixture, which may be related to the ESP's pores.

Two significant peaks were seen for the control mix sample at 1,415.94 and 971.17 wavenumbers at room temperature. The most likely functional group for the former peak, which has a wavenumber of 971.17, is an olefinic (alkene) group as trans-C—H—out of-plane bend for the later peak and a carbonyl compound as carboxylate (carboxylic acid salt) for the latter peak. Wavenumbers 1,420.67, 958.04, and 430.68 are present in the spectra of the sample with 0%ESP that was exposed at 200°C. The first peak in, this case, can be categorized as an inorganic silicate ion compound or a simple hetero-oxy compound as aromatic phosphates, while the second peak can be categorized as an inorganic carbonate ion or carbonyl compound as carboxylic acid salt (carboxylate) (P—O—C stretch). Thiols and thio-substituted molecules, such as aryl disulfide (S—S stretch), can be categorized as the third peak [35]. The following results were obtained by testing a mix that included 5%ESP utilizing an FTIR spectrum test. For 5%ESP at room temperature, the major peaks are 3,390.62 cm^{-1}, which can be categorized as alcohol and hydroxyl compounds as hydroxyl groups, H-bonded OH stretch, or normal "polymeric" OH stretch; 2,287.27 cm^{-1}, which can be categorized as common inorganic cyanide ion or carbonyl compound as transition metal carbonyls; and 1,413.97 cm^{-1}, which can be categorized as olefinic compound. In addition, the relevant functional group may be an unbound hydroxyl group (OH stretch), a nitrogen multiple bond, or a double bond complex like aliphatic cyanide or a common inorganic carbonate ion or inorganic silicate ion [2].

Even if the temperature is different in both mixtures, inorganic phosphate molecules are still present. This molecule may form as a result of a chemical reaction that takes place during mixing or because a superplasticizer was added to the mixture. Figure 17 illustrates the quantifying functional group

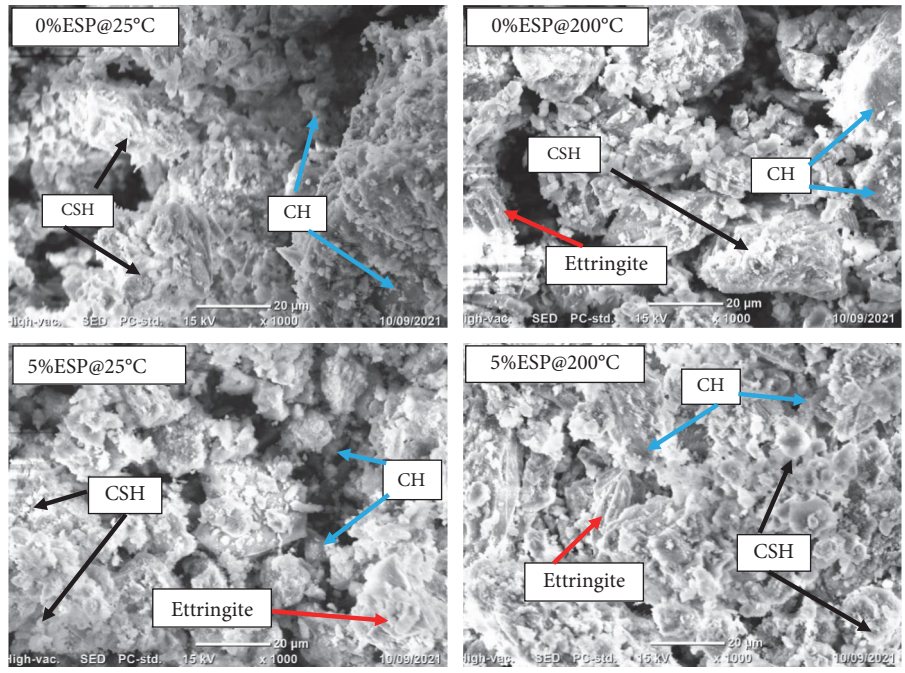

FIGURE 18: SEM image for selected 0% and 5%ESP concrete mixtures. Source: Own work, 2022.

with the degree of oxidation through identifying chemical composition/properties.

3.12. SEM Analysis. At the specified temperatures, SEM analyses revealed various differences in the morphology of control and ESP-blended concrete mixtures. Due to the reaction between C_3S and C_2S and water in the first image, both C—S—H and CH (portlandite) are present.

Due to inadequate magnification, pores are not evident in the SEM image, but the filler material has a discernible impact on the strength of the binding between particles. In contrast, pores are plainly visible in the second image, which may be a result of moisture evaporating as a result of the higher temperature. Ettringite, a needle-like structure that forms when C_4AF is hydrated and reacts with silica, was created in this instance as well. By densifying the microstructural arrangement, which is directly related to the durability attributes of the material, a decrease in the amount of pores has its own impact on the concrete quality. The third and fourth SEM images demonstrate this situation, which was created when ESP was used as a filler material in the mixture and melted between 100 and 200°C. This material may operate as a bridge in the formation of a crystal between the CH and C—S—H. Therefore, by raising microstructural integrity and resulting in better serviceability requirements, the addition of ESP up to 5% has a substantial impact. Figure 18 shows the SEM images of concrete specimens that were heated to 25 ± 2 and 200°C, respectively.

3.13. XRD Analysis. The outcome shows that the hydration of C_3S and C_2S caused a significant amount of jennite (C—S—H gel) to develop under ambient conditions. As the primary hydration product, $Ca(OH)_2$ was also produced. However, samples heated to 200°C showed a higher rate of portlandite (calcium hydroxide) synthesis, which may be related to the degradation of limestone, which is present in cement by endothermic heating and transforms to calcium oxide. A quiet quartz peak can be seen, which may be brought on by dissolved silicon dioxide. However, the value is larger in the heated sample concrete, which could be the result of temperature or pressure changes creating a quartz crystal. Generally, at 5%ESP, the finding in both SEM and XRD shows a higher degree of presence in C—S—H and CH, which are the major components affecting the microstructural integrity of concrete. Moreover, those experimental tests can clearly show the morphological and mineralogical composition of the sample concretes. The result of XRD analysis of concrete samples at 25°C and 200°C after 28 days of hydration for 0% and 5%ESP are shown in Figure 19.

The outcome shows that a significant amount of jennite (C—S—H gel) was produced at 200°C as a result of ESP melting and functioning as a filler to densify the C—S—H crystal. As the primary hydration product, $Ca(OH)_2$ was also produced. However, there are no appreciable differences in the portlandite (calcium hydroxide) development between the two sample areas. Both mixtures also had $CaCO_3$ peaks because ESP contains a lot of $CaCO_3$. Additionally, silicon dioxide is responsible for the quartz peak, but the value is higher under ambient conditions than it is under elevated temperatures. By assisting in maximizing the presence of silicon oxide, ESP could act as a heat filler and cause this scenario to occur. The findings for 5%ESP at room and 200°C temperatures are illustrated, as shown in Figure 20.

3.14. DSC Test Result of ESP. The evaporation of moisture due to temperature and forms of melted crystals may cause

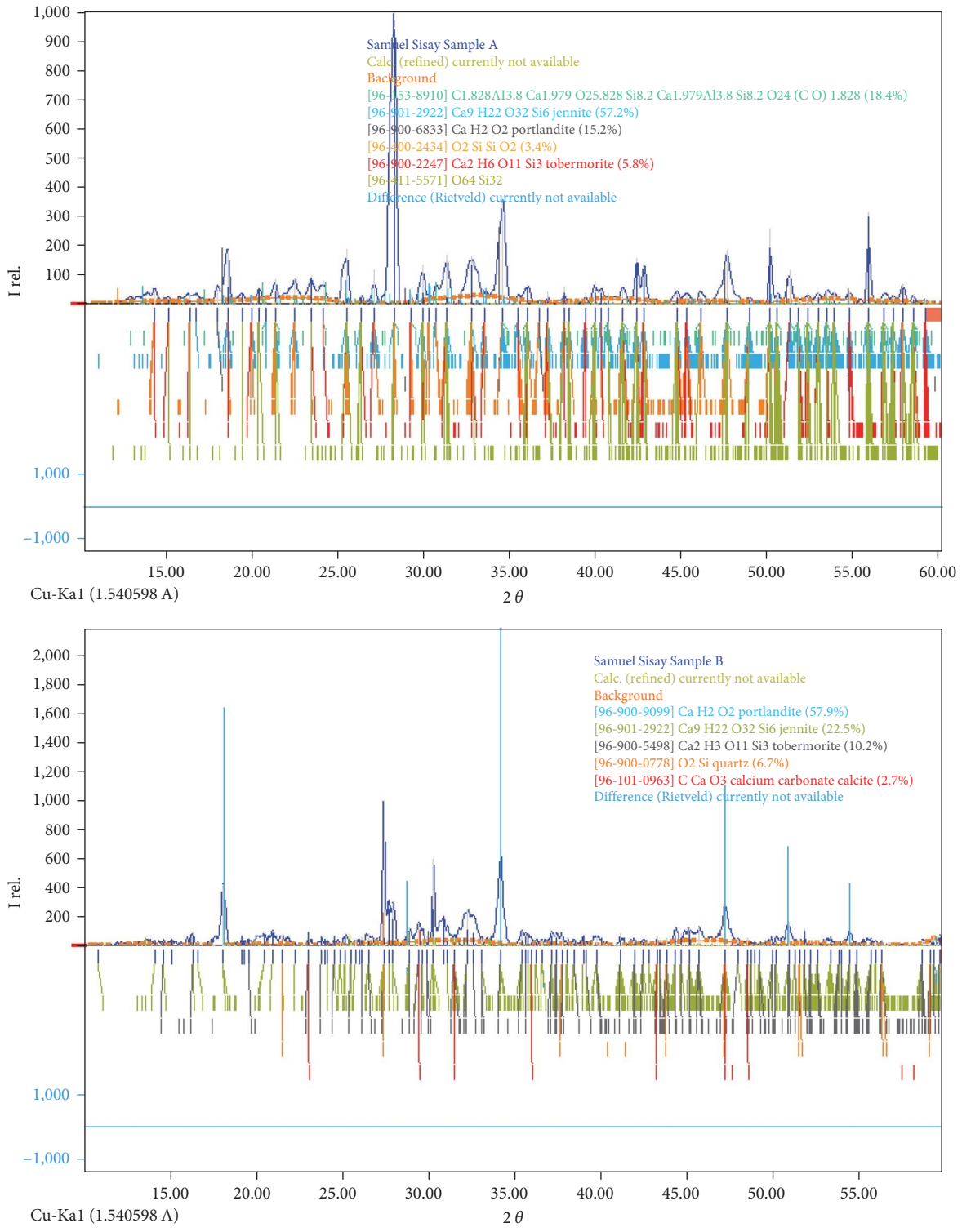

Figure 19: XRD result for 0%ESP @25 and 200°C. Source: Own work, 2022.

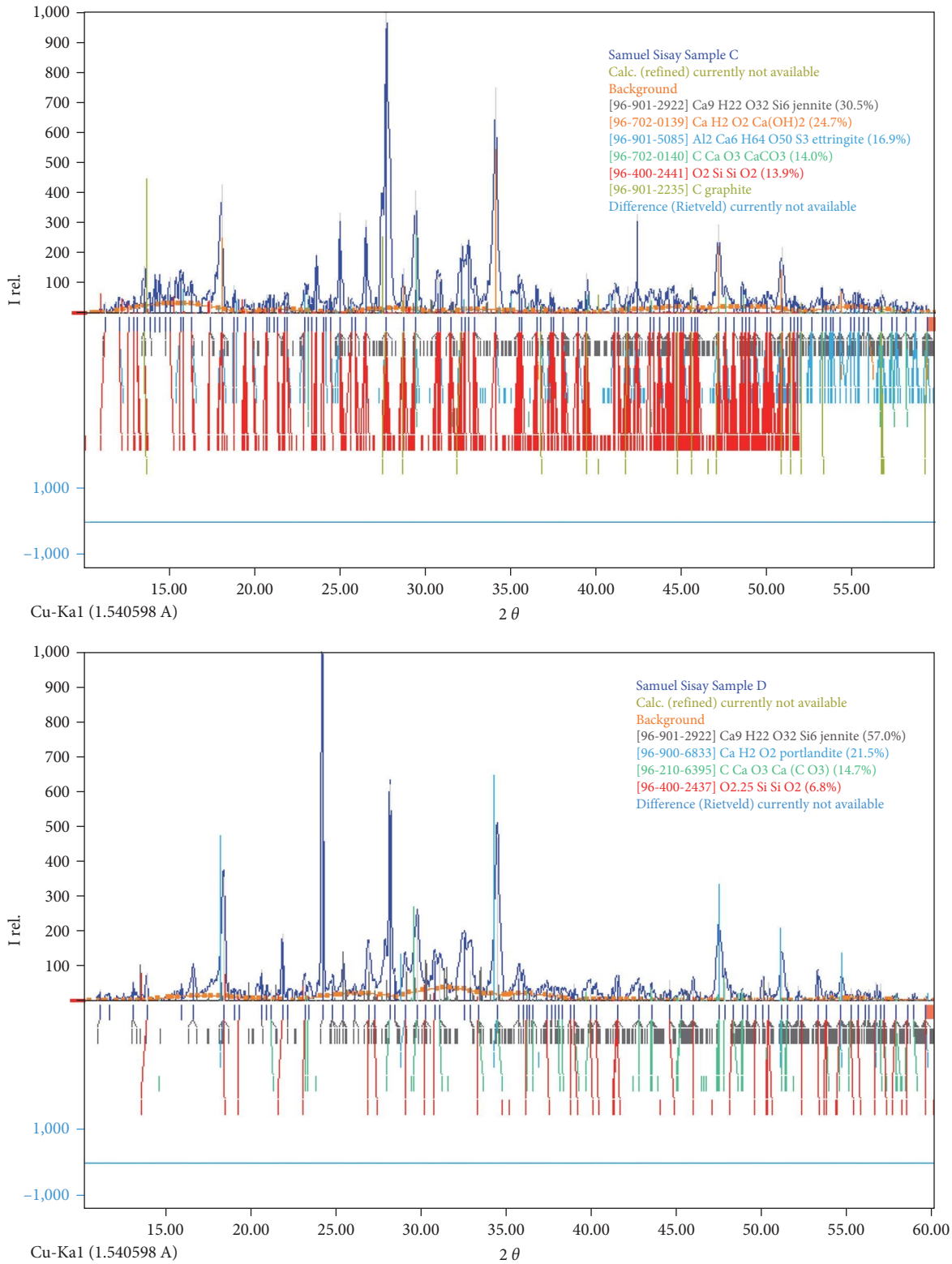

Figure 20: XRD result for 5%ESP @25 and 200°C. Source: Own work, 2022.

Table 7: Major peaks of ESP sample result (calculated using OriginPro 2019 software).

Peak ID	Peak row	Peak X	Peak Y	Peak height from baseline	Peak area	FWHM
Peak 2	3,095	337.3	3.9	7.26	925.281	88.61941
Peak 3	3,341	362.6	3.62	6.98	34.1115	2.92605
Peak 4	4,375	469.1	6.08	9.44	881.3205	102.48162
Peak 5	6,265	657.3	11.3	14.66	2335.0475	173.93667

Source: Own work, 2022.

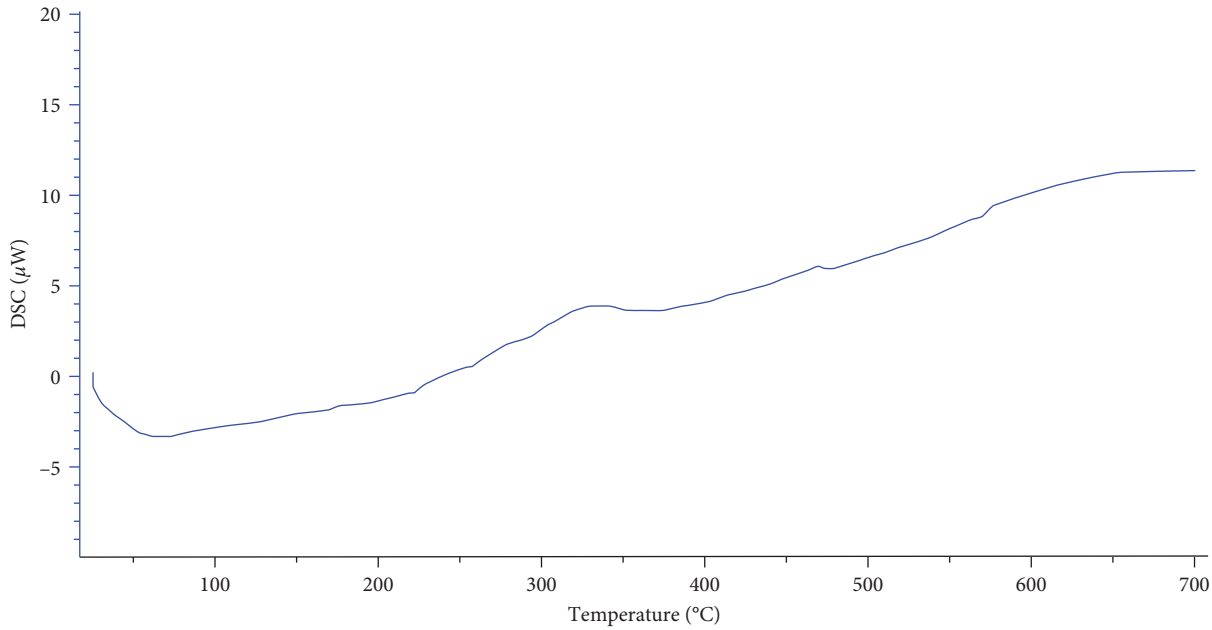

Figure 21: Heat flowing into or out of ESP sample as a function of temperature. Source: Own work, 2022.

the first peak to develop. The peaks from the exothermic area are categorized as crystallizations. Table 7 presents the major peaks of sample ESP.

The ESP's DSC curves showed an exothermic four peaks at 337.3, 362.6, 469.1, and 657.3°C and an endothermic single peak at 72.5°C for crystal melting under nitrogen gas flow, as shown in Figure 21.

4. Conclusion

Based on the experimental results and observations made, the following conclusions could be drawn:

According to the results, the workability of concrete reduces as the content of ESP rises beyond 5%ESP. This might be attributable to ESP's high water absorption rate, which depletes water and limits flowability. Additionally, the data obtained from the pressurized air content test illustrate as the presence of ESP increased the existence of free air increased up to 4.2%. This shows that the powder has pores, and those pores entrap air from the surrounding; accordingly, the strength and durability is also deteriorated as free air increases.

At room temperature, the higher UPV values were 4,230 and 4,380 m/s for the control mix and 5%ESP mix, respectively, which is classified as good in terms of concrete quality. However, a higher value was recorded at 200°C with an average UPV of 4,420 m/s, and this may be due to the melted ESP form as crystal pores filler. Surface cracks and substantial bonds between paste and aggregates were investigated. The surface bond of the concrete sample containing 5%ESP is superior to that of the control mix and the development of thick calcium hydroxide due to the presence of silica and $CaCO_3$. After heating up to 200°C,

the compressive strength of all mixtures reduced by 3.3%–8.14% compared to the strength values at the ambient temperature except for 5%ESP. At 5%ESP mix, an increase in strength occurs due to the formation of dense crystal C—S—H due to melted ESP as crystal void filler.

The increment in the amount of ESP beyond 5% has a positive relation with water absorbability of the concrete. It is obvious looking a color change when samples are immersed in an acid solution. The experimental result indicates that all specimens were affected by the acid concentration. However, better resistance to acid was observed in samples having 5%ESP.

Specimens with 0% and 5%ESP were tested for FTIR, SEM, and XRD. At both 25 and 200°C, the first mixture had little free water. The second mix, however, contains a substantial amount of free water throughout the mixture, which may be caused due to the ESP's pores. A decrease in the occurrence of pores has its own influence on the concrete quality by densifying the microstructural arrangement, which is directly related to the durability properties of the material. This scenario was obtained when ESP was substituted as a filler material in the mix and melted around 100–200°C, which may act as a bridge in forming a crystal between the CH and C—S—H, as shown in the third and fourth SEM images. The XRD data showed that the concrete specimens' mineralogy varied depending on their temperature. It results from the high-temperature disintegration of concrete.

The author suggests that conducting further studies are needed on mechanical properties like Modulus of elasticity, creeping, shrinkage, permeability, and flexural tests. It is also recommended to conduct an experimental study on ESP in terms of implementation and frequent use.

Data Availability

The corresponding author can provide the primary and secondary data utilized to support the findings of this study upon request.

Conflicts of Interest

The authors stated that the publication does not include any conflicts of interest.

Acknowledgments

The authors wish to thank MAM Bakery, Addis Ababa, Ethiopia, for providing the much-needed eggshell waste. The technical support received from Addis Ababa Science and Technology University Civil Engineering laboratory staff is also appreciated and acknowledged.

References

[1] C. Meyer, "The greening of the concrete industry," *Cement and Concrete Composites*, vol. 31, no. 8, pp. 601–605, 2009.

[2] A. Schöler, B. Lothenbach, F. Winnefeld, and M. Zajac, "Hydration of quaternary Portland cement blends containing blast-furnace slag, siliceous fly ash and limestone powder," *Cement and Concrete Composites*, vol. 55, pp. 374–382, 2015.

[3] F. Pacheco Torgal, S. Miraldo, J. A. Labrincha, and J. De Brito, "An overview on concrete carbonation in the context of eco-efficient construction: evaluation, use of SCMs and/or RAC," *Construction and Building Materials*, vol. 36, pp. 141–150, 2012.

[4] M. Schneider, M. Romer, M. Tschudin, and H. Bolio, "Sustainable cement production—present and future," *Cement and Concrete Research*, vol. 41, no. 7, pp. 642–650, 2011.

[5] S. Samad and A. Shah, "Role of binary cement including supplementary cementitious material (SCM), in production of environmentally sustainable concrete: a critical review," *International Journal of Sustainable Built Environment*, vol. 6, no. 2, pp. 663–674, 2017.

[6] H. Hordofa, "Experimental investigation on egg shell powder blended concrete," *Journal of SCRIBD*, 2019.

[7] U. N. Okonkwo, I. C. Odiong, and E. E. Akpabio, "The effects of eggshell ash on strength properties of [1] ACI 211.1," Reapproved, 2009, Standard Practice for Selecting Proportions for Normal, Heavyweight, and Mass Concrete, an ACI standard reported by ACI Committee 211,38pp, 2012.

[8] P. Narayanaswamy, M. Prakash, and K. Satyanarayanan, "Experimental study on partial replacement of cement with eggshell powder and silica fume," *Rasayan Journal of Chemistry*, vol. 10, no. 2, pp. 442–449, 2017.

[9] A. Saini, "Investigating on the properties of cement mortar containing eggshell powder as a partial replacement of cement," Retrieved August 9, 2019, from TIET Digital Repository, 2016.

[10] P. R. Kumar, R. S. Vijaya, and R. B. Jose, "Experimental study on partial replacement of cement with eggshell powder," *International Journal of Innovation in Engineering and Technology*, vol. 4, pp. 334–341, 2015.

[11] H. Binici, O. Aksogan, A. H. Sevinc, and E. Cinpolat, "Mechanical and radioactivity shielding performances of mortars made with cement, sand and egg shells," *Construction and Building Materials*, vol. 93, pp. 1145–1150, 2015.

[12] M. T. R. Jayasinghe, "Design of high strength concrete mix, Jn," *ResearchGate Journal*, 1997.

[13] I. Hager, "Behaviour of cement concrete at high temperature," *Bulletin of the Polish Academy of Sciences, Technical Sciences*, vol. 61, no. 1, 2013.

[14] J. O. Ukpata, D. E. Ewa, and J. U. Liwhuliwhe, "Effects of elevated temperatures on the mechanical properties of laterized concrete," *Journal of Nature*, 2023.

[15] E. Lubloy and G. L. Balazs, "Post heating behavior of concrete," in *International Workshop on Concrete Spalling due to Fire Exposure*, pp. 301–311, Eipzing, 2009.

[16] H. R. Dhabale and D. Telang, "The effect of elevated temperatures on the behavior of concrete materia," *International Journal for Research in Applied Science & Engineering Technology (IJRASET)*, vol. 11, 2023.

[17] M. Heikal, "Effect of elevated temperature on the physico-mechanical and micro structural properties of blended cement pastes," *Building Research Journal*, vol. 56, pp. 157–172, 2008.

[18] H. Fu, R. Mo, P. Wang et al., "Influence of elevated temperatures and cooling method on the microstructure development and phase evolution of alkali-activated slag," *Materials*, vol. 15, no. 6, Article ID 2022, 2022.

[19] K. K. Poloju, R. K. Manchiryal, and C. Rahul, "Strength studies on different grades of concrete considering fire exposure," *American Journal of Civil Engineering*, vol. 6, no. 1, pp. 16–23, 2018.

[20] Lausanne, "Fire design of concrete structures—materials," Structures and Modelling, Bulletin 38, international journal, 2007.

[21] Index mundi, "United Nations Statistics Division," 2007.
[22] D. Cree and A. Rutter, "Sustainable bio inspired limestone eggshell powder for potential industrialized applications," *ACS Sustainable Chemistry & Engineering*, vol. 3, no. 5, pp. 941–949, 2015.
[23] J. Piasta, "Heat deformations of cement paste phases and the microstructure of cement paste," *Materials and Structures*, vol. 17, pp. 415–420, 1984.
[24] M. Castellote, C. Alonso, C. Andrade, X. Turrillas, and J. Campo, "Composition and microstructural changes of cement pastes upon heating, as studied by neutron diffraction," *Cement and Concrete Research*, vol. 34, no. 9, pp. 1633–1644, 2004.
[25] ASTM C150/C150M, *Standard Specification for Portland Cement*, ASTM International, West Conshohocken, 2015.
[26] ASTM C 33/C33M-16e, *Standard Specification for Concrete Aggregates*, ASTM International, West, Conshohocken, PA, 2016.
[27] "Standard practice for selecting proportions for normal, and mass concrete," an ACI standard reported by ACI Committee 211, 38pp, 2009.
[28] British Standard Institution, "Method for determination of slump," London. BS EN 1881: Part 102, 1983.
[29] "Concrete Air Testing: Why, When, & How: An In-Depth Look".
[30] British Standard Institution, "Method of determination of compressive strength of concrete cubes," London, BS 1881: Part 116, 1983.
[31] S. Mohd Arif, O. Rokiah, M. Khairunisa et al., "Compressive strength of concrete containing eggshell powder as partial cement replacement," *IOP Conference Series: Earth and Environmental Science*, vol. 682, Article ID 012031, 2021.
[32] Q. Ma, R. Guo, Z. Zhao, Z. Lin, and K. He, "Mechanical properties of concrete at high temperature—A review," *Construction and Building Materials*, vol. 93, pp. 371–383, 2015.
[33] A. M. Neville, *Properties of Concrete*, Longman Group Ltd., London, journal of National Academies, 4th edition, 1995.
[34] O. Gencel, "Effect of elevated temperatures on mechanical properties of high-strength concrete containing varying proportions of hematite," *Fire Mater*, vol. 36, no. 3, pp. 217–230, 2012.
[35] A. B. D. Nandiyanto, R. Oktiani, and R. Ragadhita, "How to read and interpret FTIR spectroscope of organic material," *Indonesian Journal of Science & Technology*, vol. 4, no. 1, pp. 97–118, 2019.